Controlling the spatial location of photoexcited electrons in semiconductor CdSe/CdS core/shell nanorods

Chunxing She,[1] Garnett W. Bryant,[2] Arnaud Demortière,[1] Elena V. Shevchenko,[1] and Matthew Pelton[1]
[1]*Center for Nanoscale Materials, Argonne National Laboratory, Argonne, Illinois 60439, USA*
[2]*National Institute of Standards and Technology, Quantum Measurement Division and Joint Quantum Institute, Gaithersburg, Maryland 20899, USA*

(Received 13 March 2012; revised manuscript received 21 December 2012; published 22 April 2013)

It is commonly assumed that after an electron-hole pair is created in a semiconductor by absorption of a photon the electron and hole rapidly relax to their respective lowest-energy states before recombining with one another. In semiconductor heterostructure nanocrystals, however, intraband relaxation can be inhibited to the point where recombination occurs primarily from an excited state. We demonstrate this effect using time-resolved optical measurements of CdSe/CdS core/shell nanorods. For nanorods with large CdSe cores, an electron photoexcited into the lowest-energy state in the core remains in the core, and an electron photoexcited into an excited state in the CdS shell remains in the shell, until the electron recombines with the hole. This provides a means of controlling the spatial location of photoexcited electrons by excitation energy. The control over electron localization is explained in terms of slow relaxation into the lowest-energy electron state in the nanorods, on time scales slower than electron-hole recombination. The observation of inhibited relaxation suggests that a simple picture of band alignment is insufficient for understanding charge separation in semiconductor heterostructures.

DOI: 10.1103/PhysRevB.87.155427 PACS number(s): 78.67.Lt, 73.20.Jc, 73.22.−f, 78.47.D−

I. INTRODUCTION

Recent advances in colloidal synthesis have enabled the production of high-quality nanocrystals consisting of different semiconductor materials joined together in anisotropic arrangements, with epitaxial junctions between the materials.[1] These nanocrystal heterostructures provide control over the spatial localization and dynamics of electrons and holes on the nanoscale, facilitating their application as optically absorbing and emitting materials. For example, applications in photovoltaic devices and photocatalysis are improved by rapid separation of photoexcited electrons and holes into the different regions of the heterostructure.[2] By contrast, for applications where the nanocrystals emit light, including light-emitting diodes,[3] lasers,[4] and luminescent solar concentrators,[5] localization of electrons and holes in a single region is generally desirable since it leads to high recombination rates and high luminescence quantum yields.[6]

In order to determine the spatial location of electrons and holes in semiconductor heterostructures, it is often thought to be sufficient to consider only the bulk band-edge alignments of the different materials involved. For heterostructures with type-II alignment, the conduction band minimum and valence band maximum are located in different materials, leading to separation of the lowest-energy electron and hole states. For heterostructures with type-I alignment, the band extrema are located in the same material, so that the lowest-energy states of the carriers are located in the same material. A third category, sometimes referred to as "quasi-type-II," describes heterostructures in which the lowest-energy hole is localized within one material and the lowest-energy electron is delocalized throughout the heterostructure. Generally, only these lowest-energy states are considered, based on the assumption that excitation of a high-energy electron-hole pair in the nanoparticle is followed by rapid relaxation of the carriers to their respective lowest-energy states, followed by much slower electron-hole recombination.[7] This is analogous to Kasha's rule in molecular spectroscopy, which holds that excitation of a molecule into a highly excited state is followed by rapid internal conversion, so that luminescence occurs from only the lowest excited state.[8,9] Just as there are exceptions to Kasha's rule in molecular systems,[8,9] though, the assumption of rapid carrier relaxation in nanocrystals is not universally valid.[10]

Soon after studies of semiconductor nanocrystals first began, it was predicted that they should exhibit slow electron relaxation, because available phonon energies would not in general match the separation between quantum-confined electron states.[11–13] This "phonon bottleneck" is not usually observed, however, when excitons are excited in colloidal nanocrystals, because the electrons can undergo rapid relaxation, on time scales less than 1 ps, through Auger excitation of holes.[14–16] Even in the absence of holes, electron relaxation times are generally on the order of 1–10 ps, because of the presence of additional relaxation pathways, including transitions through trap states[17,18] and coupling to vibrations in organic molecules used to passivate the nanocrystals.[19] Nanosecond relaxation times were demonstrated only recently by carefully engineering the nanocrystals to eliminate these pathways.[10] Developing other, readily synthesized nanomaterials with electron relaxation times on the order of nanoseconds or longer will increase the possibility of extracting "hot" electrons; this has the potential, for example, to increase the efficiency of solar energy conversion.[20,21]

In this article we demonstrate that slow intraband relaxation in CdSe/CdS core/shell nanorods means that excitation of the nanorods at different energies can lead to different carrier localization, thus providing a method of controlling the spatial location of photoexcited electrons by excitation energy. Electrons excited into higher-energy states, which are delocalized in the nanorod, remain in a higher-energy state, regardless of the core size. By contrast, when electrons are excited into the lowest-energy state, the electrons remain localized in the CdSe cores, if the core diameter is large (∼5 nm), whereas they are

located primarily in the shell, but next to the core, if the core diameter is small (∼2 nm). We will refer to this lowest-energy electron state as the "quasicore" state, because it is excited by photons below the band gap of the CdS shell, and because it is always located near the core. We observe inhibited relaxation into this quasicore state by directly probing the location of the electrons using time-resolved optical measurements, and we corroborate the observation using theoretical calculations that show the nature of the electron states involved. Our results indicate that a description of band alignment is not necessarily adequate to determine the electron wave functions involved in optical transitions, and helps resolve the controversy[22–26] regarding the nature of this band alignment in CdSe/CdS nanocrystal heterostructures.

II. EXPERIMENTAL AND COMPUTATIONAL METHODS

Transient-Absorption (TA) Spectroscopy. TA measurements were made using a Helios spectrometer (Ultrafast Systems) coupled to an amplified Ti:sapphire laser system (Spectra-Physics, Spitfire Pro) and an optical parametric amplifier (Spectra-Physics, TOPAS).[6] For selective excitation of the quasicore states, pump-photon energies of 2.0 to 2.3 eV were used, depending on the core size. Since these wavelengths are below the CdS band gap energy, the shell is not excited. For excitation of the shell, a pump-photon energy of 3.1 eV, above the CdS band gap energy, was used. The CdSe/CdS core/shell NRs studied, which were synthesized according to previously published procedures,[6] have shell volumes at least 20 times greater than their core volumes, ensuring that the great majority of the absorption at 3.1 eV is into the shell. Pump pulse energies were maintained at 20 to 50 nJ per pulse, low enough that less than one electron-hole pair is generated on average per nanorod per laser pulse.[6] The samples were rapidly stirred during the measurements to avoid any cumulative effects due to sample heating or charging. Measurements of absorption spectra verified that the samples were not damaged during the transient-absorption measurements. Transmission-electron-microscope images of the NR samples show highly uniform nanorods, with no evidence of a byproduct of CdSe only or thin-shell nanocrystals.[6]

Photoluminescence (PL) Spectra and PL Decay Measurements. PL spectra were collected on a spectrofluorimeter (Jobin-Yvon Horiba, NanoLog) with an excitation energy of 2.57 eV. PL decay rates were measured as a function of emission energy by time-correlated single-photon counting (TCSPC) on the spectrofluorimeter. The samples were excited using a pulsed diode laser with a photon energy of 2.57 eV, corresponding to excitation of the quasicore states. Emitted light was filtered spectrally using a grating spectrometer before being detected with a photomultiplier tube.

Electronic Structure Calculations. We employed an sp^3d^5 empirical tight-binding (TB) theory to estimate the electron and hole states in CdSe/CdS core/shell nanorods. This provides an atomistic theory with an unambiguous modeling of the effects of dot size, shape, and variations in composition on the monolayer scale. Models similar to the one we use here have been employed to accurately describe the electronic states of both III-V and II-VI homogeneous nanocrystals, nanocrystals under hydrostatic pressure, and highly strained core-shell structures with shell thicknesses down to a single monolayer.[27–29]

A nine-state atomiclike basis set (s; x; y; z; xy; yz; xz; x^2-y^2; $3z^2$-r^2) was used to describe each atom in the structure, and interactions were restricted to nearest neighbors only. The inclusion of d orbitals in the minimal basis set is necessary to provide a good description of the bulk band dispersion at high symmetry points at the edge of the Brillouin zone.[30] This is important in small structures and in highly strained structures, where mixing of states away from the center of the Brillouin zone is needed to describe strongly confined states. Spin-orbit interactions were described by including only the contributions from the p states; the much smaller splittings of excited d states were neglected. In order to mimic the effects of surface passivation by ligands and to eliminate spurious surface states lying inside the gap, we shifted the energies of the sp^3 dangling-bond orbitals on the surface atoms well above the conduction band edge.[27–29,31] Dangling bonds due to d states do not contribute to the gap states.

TB parameters taken from Ref. 32 were changed slightly to better reproduce the bulk band gaps,[28] and the CdSe/CdS band offsets were obtained from Ref. 33. The cores and shells were modeled as cylindrical nanorods with hemispherical ends, with dimensions chosen to correspond to the NRs measured in Fig. 1 of the main text, and with the core located one-third of the way from one end of the shell.[23] We verified using additional calculations that the results are qualitatively unchanged by variations in the position of the core within the shell.

We began with the atoms in the core-shell structure initially located on the regular lattice of the uniform core material. Such a uniform system exhibits enormous strain, because the atoms in the shell are far from their bulk positions. We minimized the strain energy by relaxing the lattice using the valence-force-field method.[27,34,35] In this method the atoms in the core and shell are allowed to move in any direction in order to achieve strain relaxation at the interfaces. Minimization of the strain energy was performed using a combination of steepest-descent and conjugate-gradient techniques. The relaxed atomic positions produce local changes of the bulk tight-binding matrix elements between neighboring atoms (off-site TB parameters V_{kl}). The effects of the relaxed bond angles and atomic positions on the TB matrix elements were calculated using the Slater-Koster formulas;[36] power-law scaling is used for the changed bond lengths $V_{kl} = V^0_{kl}(d^0_{ij}/d_{ij})^k$, where d_{ij} is the bond length between the nearest neighbors i and j, and the superscript 0 refers to the unstrained values. A single exponent is sufficient because, in the sp^3d^5 parametrization proposed by Sarma,[32] the hopping parameters obey the universal Harrison scaling law $\kappa = 2$, ensuring transferability to the nanocrystals. The scaling-law exponent can also be determined empirically by comparing calculated bulk band edges under hydrostatic strain to experimental values of the deformation potential.[28] Values for the exponent other than the Harrison scaling law can sometimes give better electronic structure,[29] and uncertainty in the bulk deformation potential can lead to uncertainty in the exponent. To account for these possibilities, we have considered larger values of κ, and found that the results did not change qualitatively. Most importantly for the issues discussed here, the character and localization of the lowest electron and hole states were unchanged. Once the nanocrystal structure

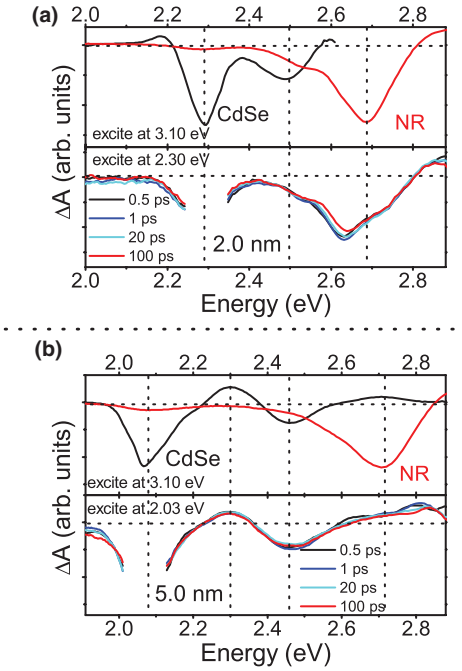

FIG. 1. (Color online) Transient spectra for CdSe/CdS core/shell nanorods (NRs). (a) Spectra for NRs with 2-nm cores (nanorod volume $V = 570$ nm^3, length $L = 43$ nm, diameter $D = 4.1$ nm). (b) Spectra for NRs with 5-nm cores ($V = 550$ nm^3, $L = 38$ nm, $D = 4.3$ nm). The bottom panels show spectra for excitation of the lowest-energy, quasicore state with a pump-photon energy of 2.30 eV (for 2-nm cores) or 2.03 eV (for 5-nm cores) and for pump-probe delay times of 0.5, 1, 20, and 100 ps. The top panels show spectra for excitation of the CdS shell with a pump-photon energy of 3.10 eV and a pump-probe delay time of 2.0 ns. Also shown for comparison are transient spectra for bare CdSe nanocrystals with the same dimensions as the cores of the NRs. The CdSe spectra have been shifted downwards in energy by 0.26 eV (for 2-nm cores) and by 0.04 eV (for 5-nm cores), for easier comparison to the bottom panels; these shifts correspond to the reduction in the CdSe transition energies in the NRs as compared to the bare CdSe particles, based on their linear absorption spectra. The portions of the transient spectra near the pump-photon energies are dominated by scattered pump light, and have therefore been excluded from the graphs.

was defined, we found the single-particle electron and hole eigenvalues by diagonalizing the TB Hamiltonian using an iterative solver.

Since the purpose of the calculations is simply to provide a qualitative explanation of the observed electron localization, we ignore the effects of electron-hole interaction on the carrier wave functions. These interactions are not expected to qualitatively modify the nature of the electron states in the NRs, as is evidenced by the consistency between experiments and theory shown below. These interactions will, however, shift the energies of optical transitions; we provide an estimate of this shift in order to simplify comparison between calculated spectra and experimental results. The electron-hole interaction energy is estimated based on the bulk dielectric constant and on the average separation between a given electron state and a hole localized in the CdSe core.

III. RESULTS

A. Transient-absorption measurements

Transient-absorption measurements of the core/shell NRs provide information about the location of electrons in the heterostructures.[7] If an electron is located in the core of an NR, it blocks the creation of electron-hole pairs in the core; this is reflected as a reduction in the absorption of the probe light—that is, a negative transient-absorption peak, or bleach signal—near the CdSe band edge. Similarly, if an electron is located in the shell of a NR, it produces a bleach signal near the CdS band edge. Holes are rapidly trapped into the core due to the high density of closely spaced hole states and the large valence-band offset between CdSe and CdS, so that any changes in the transient-absorption bleach signal more than a few picoseconds after the pump pulse are due to electrons alone.[6,37] All of the NRs that we measured have high photoluminescence quantum yields (10%–50%), indicating that trapping of carriers in surface states does not play a dominant role in their optical properties.

The top panels of Figs. 1(a) and 1(b) show transient spectra (red curves) for NRs when the shells are excited with a pump-photon energy of 3.10 eV. Photons with these high energies are much more likely to be absorbed by the large CdS shell than the small CdSe core, so that the resulting transient-absorption signal is dominated by electrons that have been created in the shell. The CdSe/CdS nanorods[6,22,23] used herein have two different core sizes: The first, referred to as 2-nm core, have a spherical core with a diameter of 2.0 ± 0.2 nm, and the second, referred to as 5-nm core, have a prolate spheroidal core with a polar diameter of 5.0 ± 0.5 nm and an equatorial diameter of 3.0 ± 0.3 nm. We compare nanorods with similar volumes since previous work has shown that volume is related to electron-hole overlap when the shell is excited.[6]

The spectra show a distinct peak at the CdS band-edge energy, near 2.7 eV, and a much smaller peak at the CdSe band-edge energy, near 2.3 eV. The energies of these bleaches correspond to those of the absorption peaks of CdS and CdSe in the absorption spectra.[6,37] Representative data are shown for delay times of 2 ns; transient spectra at shorter delay times and longer delay times, up to the 20-ns electron-hole recombination time, showed the same features. Similar transient spectra are also obtained when the pump-photon energy is 2.70 eV, corresponding to direct excitation of the CdS band-edge transition. This indicates that when the shell is excited the relaxed electrons remain primarily in the shell until they recombine with holes. More details about transient spectra and transient kinetics under these excitation conditions have been given in previous publications.[6,37] For comparison, the top panels also show transient spectra obtained from bare CdSe nanocrystals. In this case, there are two bleaches at energies distinct from the CdS transition energy. These two features correspond to transitions in the quasispherical CdSe nanocrystals between the lowest-energy electron state and the two lowest-energy hole states that couple strongly optically to the electron.

The bottom panel of Fig. 1(a) shows the transient spectra that are obtained when CdSe/CdS core/shell NRs with 2-nm cores are excited with a photon energy of 2.30 eV, corresponding to excitation of the quasicore state. The largest

peak occurs near the CdS band-edge energy (at 2.62 eV), indicating that the relaxed electron is partially in the shell and can couple with hole states in the CdS shell. There is also a peak at the lowest CdSe transition energy (2.30 eV), indicating that the relaxed electron is partially in the core and can couple to CdSe hole states. (The higher-energy CdSe transition at approximately 2.5 eV is largely absent, indicating that the higher-energy hole states in these core/shell nanorods are different from those in bare CdSe nanocrystals.) Thus, the transient spectra in Fig. 1(a) clearly indicate that two different electron states are involved for different excitation energies, one with a higher degree of delocalization and a higher energy indicated by the CdS bleach at 2.69 eV (top panel), the other with a lower degree of delocalization and a lower energy indicated by the CdS bleach at 2.62 eV (bottom panel).

By contrast, the bottom panel of Fig. 1(b) shows qualitatively different behavior when NRs with 5-nm cores are excited at the CdSe transition energy of 2.03 eV. In this case, the spectrum is nearly identical to that of bare CdSe, with two bleach features at approximately 2.1 and 2.45 eV that reproduce the two transitions in the bare CdSe nanocrystals. No peak at the higher, CdS transition energy is visible. This indicates that the electron is localized within the CdSe core, demonstrating that the state of the electron in these NRs depends on the excitation energy that is used.

Figure 2 shows the time dependence of the bleach signals probed at different energies within 10 ps after excitation of the cores. All signals rise instantaneously (within the approximately 150 fs instrument time resolution) and remain constant thereafter. The independence of the kinetics on probe-photon energy is an indication that, for each NR sample, a single electron state is responsible for the observed transient bleach. The instantaneous rise indicates that these electron states are populated directly by the pump laser, without any intermediate relaxation or charge-transfer processes.

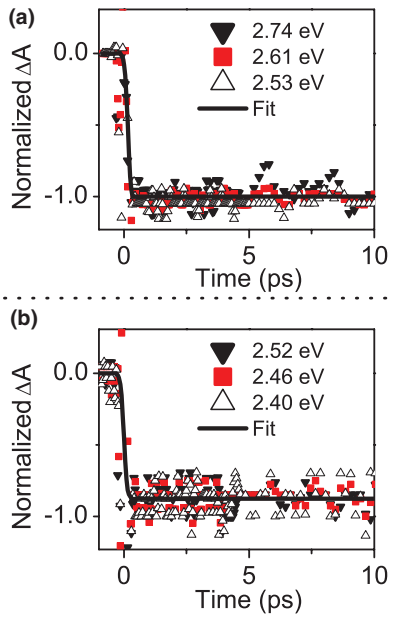

FIG. 2. (Color online) Transient kinetics for CdSe/CdS core/shell nanorods following excitation of the CdSe cores, for NRs with (a) 2-nm and (b) 5-nm cores. Kinetics are shown for different probe-photon energies around the bleach of CdS and CdSe in the bottom panels of Fig. 1, and are normalized by their value at 1 ps. The fits are step functions convolved with the 150-fs instrument response function.

The TA measurements thus demonstrate that exciting the NRs with photon energies above the CdS band gap results in an electron in a higher-energy state that is located mainly in the shell and that does not relax into the lowest-energy, quasicore state. The quasicore state, with delocalization/localization dependent on the core size, is accessible only by exciting the electron directly into that state.

B. Time-resolved photoluminescence measurements

Further evidence for this core-size-dependent localization of the lowest-energy state comes from photoluminescence (PL) decay measurements. According to Fermi's golden rule, spontaneous emission rates increase with the overlap between the electron and hole wave functions and with the energy of the emitted photon.[38] Comparing emission rates at the same photon energy for different samples thus provides a measure of the relative electron-hole overlap among the samples. Since low-energy hole states are always localized in the cores,[6,37] the PL lifetimes indicate the degree to which the electron is localized in the core or delocalized in the shell.

Figure 3(a) shows emission spectra for samples with different core and shell sizes excited with a photon energy of 2.57 eV, corresponding to excitation of the quasicore states. For NRs with 5-nm cores, the decay rate at a given energy is nearly

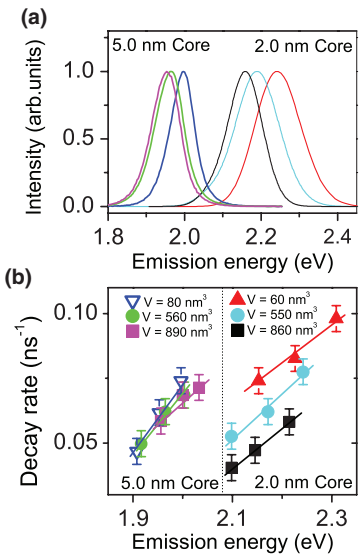

FIG. 3. (Color online) (a) Emission spectra of CdSe/CdS core/shell nanorods when exciting the CdSe cores with a pump-photon energy of 2.57 eV. The three spectra on the left are for nanorods with 5-nm cores, and the three on the right are for nanorods with 2-nm cores. The nanorod volumes V are 890, 560, 80, 860, 550, and 60 nm^3, from the left to the right. (b) Photoluminescence decay rates as a function of emission energy, for the same nanorods as in (a). Decay rates are estimated as the inverse of the $1/e$ decay time of the time-resolved photoluminescence signal. Symbols are experimental data and solid lines are guides for the eye. The error bars represent 10% uncertainty.

independent of shell size, as shown in Fig. 3(b). This strongly suggests that both radiative and nonradiative recombination rates remain constant since, otherwise, the change in one would need to exactly cancel the change in the other. A constant radiative recombination rate, in turn, means that the overlap between the electron and hole wave functions is constant, corresponding to spatially direct recombination between an electron and a hole both localized within the core.

By contrast, for NRs with 2-nm cores, the decay rate decreases dramatically as the shell gets larger, indicating spatially indirect recombination between a hole localized in the core and an electron partially in the shell. We have previously seen that when the shell is excited decay rates always decrease as the shell gets larger, regardless of the size of the core.[6] Comparison to measurements of quantum yield indicated that this decreasing decay rate is due to a decrease in radiative recombination, rather than a change in nonradiative recombination.[6] This means that the overlap between the electron and hole wave functions decreases as the shell gets larger, corresponding to delocalization of electrons in the shell.

Together, the transient-absorption measurements and the PL decay measurements provide unambiguous evidence that two different electron states, one with higher energy and the other with lower energy, are involved in optical transitions following excitation of the shells and the quasicore states, respectively. An electron in the higher-energy state is inhibited from relaxing into the lower-energy state within the approximately 10–20 ns that it takes for the electron to recombine with the hole. The experiments also clearly demonstrate that the state accessed by excitation of the quasicore remains primarily localized around the core—inside the core when it is larger and partially in the shell when the core is smaller—whereas the state accessed by excitation of the shell remains primarily delocalized in the shell.

C. Electronic structure calculations

To gain more insight into the nature of the states involved in the optical transitions, we calculated electron and hole states in the NRs using an empirical tight-binding theory.[27–29] As expected, the calculations show that there are multiple low-energy hole states localized within the CdSe cores, regardless of core size. For electrons, by contrast, there is at most one lowest-energy state localized in the core, as shown in Fig. 4. For NRs with 2-nm cores, neither the lowest-energy electron state (E1) nor the second-lowest-energy electron state (E2) are located in the core. E1 is located around the core, but mostly in the shell, having only 9% of its electron density in the CdSe core, and E2 has less than 1% of its electron density in the core. For NRs with 5-nm cores, E2 is still located almost entirely in the shell, with less than 1% of its electron density in the core. On the other hand, the electron density of E1 is located almost entirely within the 5-nm core.

The correspondence between the calculated electron states and the experimental results can be further illustrated by calculating the energies and oscillator strengths of the transitions between E1 or E2 and the lowest-energy hole states in the NRs. Only these two electron states are required to explain our observations (unlike the tens of states considered in a previous study[37]). On the other hand, we consider transitions between

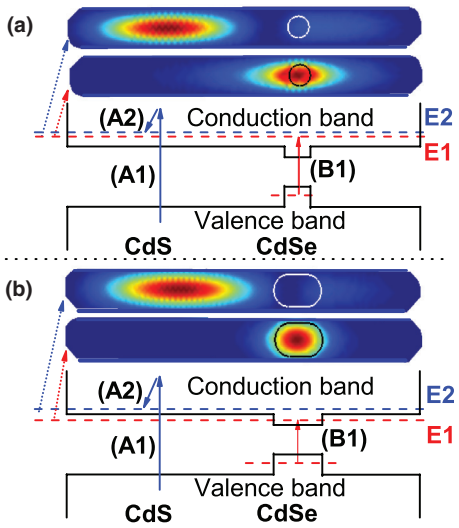

FIG. 4. (Color) Calculated electron densities for the two lowest-energy electron states, E1 and E2, in CdSe/CdS core/shell nanorods with (a) 2-nm and (b) 5-nm cores. Red indicates high density and blue indicates low density. The locations of the cores are indicated with white or black outlines. Also illustrated are the band diagrams of the nanorods and the processes involved in excitation into different electron states.

these electron states and multiple hole states, taking into account up to 39 of the lowest-energy hole states in the NRs. Figures 5(a) and 5(b) show the calculated spectra. In order to compare them more directly with the experimental transient spectra, the transitions were shifted by the estimated electron-hole binding energy and were broadened by the measured PL linewidths. The broadened and shifted spectra (red curves) are also shown in Figs. 5(a) and 5(b), and the corresponding transitions are illustrated in Figs. 5(c) and 5(d). Also shown in Figs. 5(a) and 5(b) are representative transient-absorption spectra, reproduced from Fig. 1, for comparison. As can be seen, the calculated spectra reproduce the main features of the experimental transient spectra, with small differences between calculated and measured transition energies. These energy differences may be related to the assumed offset between the CdSe and CdS valence-band edges: A wide range of values have been reported in the literature for this offset,[33,39,40] and it is expected to depend on crystal structure and orientation. Excitonic effects beyond our rough estimate of electron-hole binding may also account for differences between measured and calculated transition energies.

There also appears to be a small peak in the calculated spectrum for E1 transitions in NRs with 5-nm cores, labeled as (3) in Fig. 5(b), that is not observed experimentally. This feature is due to a large number of weak transitions involving closely spaced hole states near the CdS band edge. Additional inhomogeneous broadening not included in the model or the effects of surface roughness or surface charges (see below) would reduce the visibility of these transitions, which may explain why it is not observed experimentally. Moreover, the Stark effect in CdSe can lead to a positive feature in this region, which will also hinder the observation of this relatively small bleach feature.

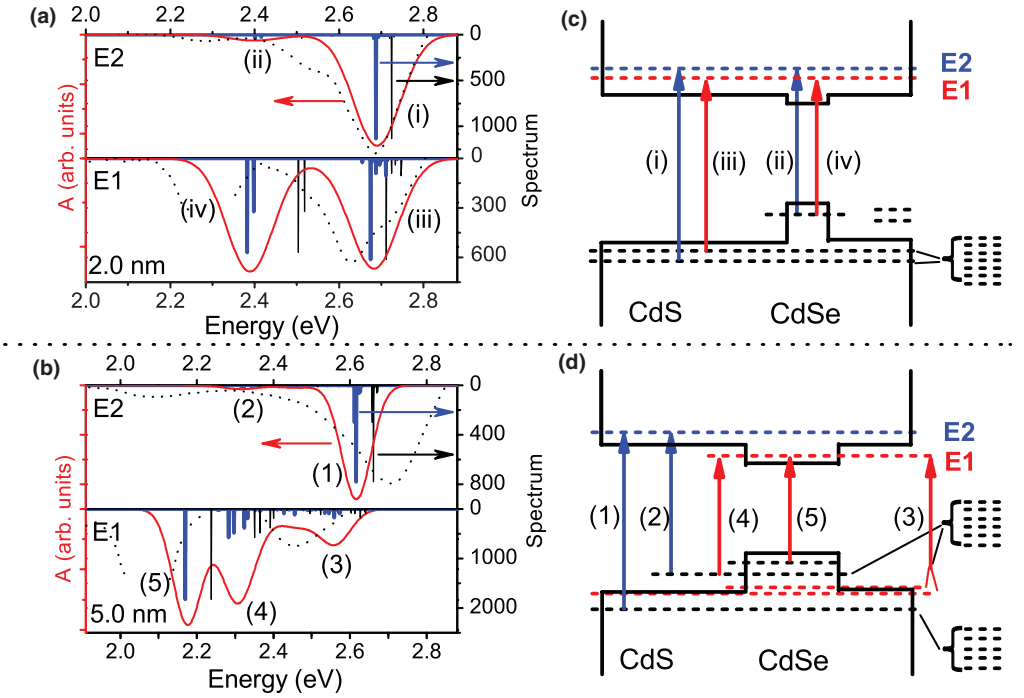

FIG. 5. (Color online) Calculated spectra for CdSe/CdS core/shell nanorods with (a) 2-nm and (b) 5-nm cores. The corresponding band structure diagrams and transitions are shown schematically in (c) and (d), respectively. Only the transitions from hole states to the two lowest-energy electron states, E1 or E2, are calculated. In (a) and (b), the thin black lines correspond to transitions calculated without considering electron-hole interactions, and the thick blue lines show the transitions shifted by estimated exciton binding energies. The red lines are calculated by broadening the shifted spectra by values corresponding to the luminescence linewidths. The dotted black lines are representative experimental transient-absorption spectra, reproduced from Fig. 1, for comparison to the theoretical spectra. The short dashed lines in (c) and (d) indicate that certain hole states represented by the long dashed lines actually correspond to groups of several, closely spaced states.

Apart from these differences, the calculated spectra for transitions involving E2 closely reproduce experimental transient spectra for excitation of the shell, and the calculated spectra for E1 reproduce experimental spectra for excitation of the quasicore states. The calculations thus support the interpretation that excitation of the shell results in electrons in E2 and excitation of the quasicore leads to electrons in E1. It appears that excitation of high-energy electron-hole pairs in the shell (process A1 in Fig. 4) is followed by rapid relaxation of the electron into E2 (process A2); however, further relaxation into E1 is very slow, so that the electron in E2 recombines with a hole before relaxing into E1. Excitation of the quasicore, by contrast, results directly in an electron in E1 (process B1), where it remains until it recombines with the hole.

IV. DISCUSSION

The current calculations do not provide electron relaxation rates, so they do not directly indicate why relaxation from E2 to E1 is slow. The slow relaxation occurs in the presence of holes, indicating that Auger relaxation must be suppressed, consistent with the report of suppressed Auger recombination in a similar system.[41] In addition, the nanocrystals are capped with standard ligand molecules, but do not appear to relax by coupling to vibrational modes in the ligands. In other words, the mechanisms usually invoked for rapid intraband relaxation of electrons do not seem to apply in this case, and we do not need to deliberately remove these mechanisms in order to observe slow relaxation in these nanocrystal heterostructures.[19]

Our calculations show that the overlap in electron density between E2 and E1 is small due to the need for orthogonality among electron wave functions. This low overlap may be at least part of the reason for the slow relaxation; in particular, it is likely to inhibit Auger scattering from E2 to E1. Additional mechanisms that are not included in the calculation may further reduce the rate of relaxation from E2 to E1,[42] including dipole shifts due to the polar interface between the two semiconductor materials,[43] and further localization of E2 within the shell due to fluctuations in the diameter of the shells or localized charges on the shell surfaces. Determining the mechanism for the electron relaxation bottleneck remains a topic for future research; single-particle measurements, in particular, have the potential to provide additional insight into the mechanism by removing the complicating effects of inhomogeneous broadening. Our current results nonetheless demonstrate that such a bottleneck exists in CdSe/CdS core/shell nanorods.

Our observation of inhibited electron relaxation resolves seemingly conflicting reports about the spatial location of the electron in CdSe/CdS core/shell nanorods: The apparent disagreement among these measurements is due to the fact that they access different electron states. The lowest-energy electron state in the nanorods is localized in large cores, and is mostly located in the shell for NRs with smaller cores. The second-lowest-energy state, by contrast, is always delocalized in the shell, away from the lowest-energy state.

The experimental results will therefore depend on which state is excited and on the size of the core. Previous TA studies, for example, involved only nanocrystals with cores smaller than 3 nm, and thus observed electron delocalization in the shell.[37] Scanning-tunneling-microscopy measurements, on the other hand, directly probed the lowest-energy states in cores larger than 3 nm, and found that they were localized in the cores.[25] Cross-polarized transient-grating measurements involved direct excitation of the lowest-energy states, which were found to be only partially delocalized into the shell.[44] Observations of strong quantum-confined Stark shifts[24] and of photocatalytic hydrogen production when the tips of the NRs are decorated with Pt[45] involved excitation of higher-energy electron states, and are consistent with delocalized electrons in the shells. One exception is a multiexciton spectroscopy study that involved excitation of the shells and nonetheless indicated a transition from electron delocalization to electron localization when the core is larger than 2.8 nm in diameter;[26] in this case, though, efficient multicarrier relaxation processes may remove any relaxation bottleneck to the lowest-energy ground state.

Our measurements are also consistent with previous measurements on different nanocrystal heterostructures that have suggested that electrons can have relaxation times comparable to recombination times. For example, CdSe/CdS core/shell tetrapods have exhibited luminescence from higher-energy transitions that appear to involve unrelaxed electrons.[46] Emission from higher-energy transitions has also been observed for heterostructures that have been engineered to provide two spatially separate potential minima for carriers;[47,48] for CdSe/ZnS/CdSe core/shell/shell nanocrystals, in particular, transient-absorption measurements also provide evidence for inhibited electron relaxation.

V. CONCLUSIONS

In conclusion, we have found that relaxation of electrons to their lowest-energy states in CdSe/CdS core/shell nanorods is inhibited to the point that it is slower than electron-hole recombination. As a result, the spatial location of photoexcited electrons can be controlled in the NRs through the choice of excitation energy. The inhibited relaxation occurs in the presence of holes, without any deliberate attempt having been made to eliminate fast relaxation pathways. Our observations also show that the band-alignment picture that is generally invoked to explain whether the electron is localized in the core (type-I alignment) or is delocalized into the shell (quasi-type-II alignment) is not sufficient to understand different experiments, because the experiments do not all probe the lowest-energy electron states in the conduction band.

Excitation of the shell of the NRs results in an electron in a higher-energy state that is located in the shell, and which does not, over several nanoseconds, relax to the lowest-energy state. Since holes are localized in the core, this means that the electron and hole are spatially separated, even if there is a lower-energy electron state available in the core. This charge separation, in turn, reduces recombination rates and increases the prospects for extraction of the electron and hole, and thus has important implications both for light emission and for solar-energy conversion. Similar relaxation bottlenecks are likely to exist in other nanocrystal heterostructures, meaning that application of these materials must involve careful attention to the process by which the electrons are excited.

ACKNOWLEDGMENTS

We thank S. B. Darling, D. H. Potterveld, and R. J. Holt for initiating the project that led to this work, M. S. Hybersten for helpful discussions, and D. Gosztola for assistance with transient-absorption measurements. Use of the Center for Nanoscale Materials was supported by the US Department of Energy, Office of Science, Office of Basic Energy Sciences, under Contract No. DE-AC02-06CH11357. Any mention of product names in this paper is solely to specify how the work was done and does not constitute endorsement or validation by NIST.

[1] P. O. Anikeeva, J. E. Halpert, M. G. Bawendi, and V. Bulović, Nano Lett. **9**, 2532 (2009).
[2] D. V. Talapin, J. S. Lee, M. V. Kovalenko, and E. V. Shevchenko, Chem. Rev. **110**, 389 (2010).
[3] J. Bomm, A. Büchtemann, A. J. Chatten, R. Bose, D. J. Farrell, N. L. A. Chan, Y. Xiao, L. H. Sloof, T. Meyer, A. Meyer, W. G. J. H. M. van Sark, and R. Koole, Sol. Energy Mater. Sol. Cells **95**, 2087 (2011).
[4] S. S. Lo, T. Mirkovic, C. H. Chuang, C. Burda, and G. D. Scholes, Adv. Mater. **23**, 180 (2011).
[5] V. Sholin, J. D. Olson, and S. A. Carter, J. Appl. Phys. **101**, 123114 (2007).
[6] C. X. She, A. Demortière, E. V. Shevchenko, and M. Pelton, J. Phys. Chem. Lett. **2**, 1469 (2011).
[7] V. I. Klimov, J. Phys. Chem. B **104**, 6112 (2000).
[8] P. Klán and J. Wirz, *Photochemistry of Organic Compounds: From Concepts to Practice* (Wiley-Blackwell, West Sussex, UK, 2009), Vol. 40, Chap. 2.
[9] M. Kasha, Discuss. Faraday Soc. **9**, 14 (1950).
[10] A. Pandey and P. Guyot-Sionnest, Science **322**, 929 (2008).
[11] H. Benisty, C. M. Sotomayor-Torres, and C. Weisbuch, Phys. Rev. B **44**, 10945 (1991).
[12] U. Bockelmann and G. Bastard, Phys. Rev. B **42**, 8947 (1990).
[13] T. Inoshita and H. Sakaki, Physica B **227**, 373 (1996).
[14] A. L. Efros, V. A. Kharchenko, and M. Rosen, Solid State Commun. **93**, 281 (1995).
[15] E. Hendry, M. Koeberg, F. Wang, H. Zhang, C. D. Donegá, D. Vanmaekelbergh, and M. Bonn, Phys. Rev. Lett. **96**, 057408 (2006).
[16] L. W. Wang, M. Califano, A. Zunger, and A. Franceschetti, Phys. Rev. Lett. **91**, 056404 (2003).
[17] D. F. Schroeter, D. J. Griffiths, and P. C. Sercel, Phys. Rev. B **54**, 1486 (1996).
[18] P. C. Sercel, Phys. Rev. B **51**, 14532 (1995).
[19] P. Guyot-Sionnest, B. Wehrenberg, and D. Yu, J. Chem. Phys. **123**, 074709 (2005).

[20]R. T. Ross and A. J. Nozik, J. Appl. Phys. **53**, 3813 (1982).
[21]W. A. Tisdale, K. J. Williams, B. A. Timp, D. J. Norris, E. S. Aydil, and X. Y. Zhu, Science **328**, 1543 (2010).
[22]D. V. Talapin, J. H. Nelson, E. V. Shevchenko, S. Aloni, B. Sadtler, and A. P. Alivisatos, Nano Lett. **7**, 2951 (2007).
[23]L. Carbone, C. Nobile, M. Dr Giorgi, F. Della Sala, G. Morello, P. Pompa, M. Hytch, E. Snoeck, A. Fiore, I. R. Franchini, M. Nadasan, A. F. Silvestre, L. Chiodo, S. Kudera, R. Cingolani, R. Krahne, and L. Manna, Nano Lett. **7**, 2942 (2007).
[24]J. Muller, J. M. Lupton, P. G. Lagoudakis, F. Schindler, R. Koeppe, A. L. Rogach, J. Feldmann, D. V. Talapin, and H. Weller, Nano Lett. **5**, 2044 (2005).
[25]D. Steiner, D. Dorfs, U. Banin, F. Della Sala, L. Manna, and O. Millo, Nano Lett. **8**, 2954 (2008).
[26]A. Sitt, F. Della Sala, G. Menagen, and U. Banin, Nano Lett. **9**, 3470 (2009).
[27]J. G. Díaz and G. W. Bryant, Phys. Rev. B **73**, 075329 (2006).
[28]J. G. Díaz, M. Zieliński, W. Jaskólski, and G. W. Bryant, Phys. Rev. B **74**, 205309 (2006).
[29]J. G. Díaz, G. W. Bryant, W. Jaskólski, and M. Zieliński, Phys. Rev. B **75**, 245433 (2007).
[30]J. M. Jancu, R. Scholz, F. Beltram, and F. Bassani, Phys. Rev. B **57**, 6493 (1998).
[31]G. W. Bryant and W. Jaskólski, J. Phys. Chem. B **109**, 19650 (2005).
[32]S. Sapra, N. Shanthi, and D. D. Sarma, Phys. Rev. B **66**, 205202 (2002).
[33]S. H. Wei and A. Zunger, Appl. Phys. Lett. **72**, 2011 (1998).
[34]T. Saito and Y. Arakawa, Physica E **15**, 169 (2002).
[35]C. Pryor, J. Kim, L. W. Wang, A. J. Williamson, and A. Zunger, J. Appl. Phys. **83**, 2548 (1998).
[36]J. C. Slater and G. F. Koster, Phys. Rev. **94**, 1498 (1954).
[37]M. G. Lupo, F. Della Sala, L. Carbone, M. Zavelani-Roddi, A. Fiore, L. Lüer, D. Polli, R. Cingolani, L. Manna, and G. Lanzani, Nano Lett. **8**, 4582 (2008).
[38]A. F. van Driel, G. Allan, C. Delerue, P. Lodahl, W. L. Vos, and D. Vanmaekelbergh, Phys. Rev. Lett. **95**, 236804 (2005).
[39]A. H. Nethercot, Jr., Phys. Rev. Lett. **33**, 1088 (1974).
[40]A. Pandey and P. Guyot-Sionnest, J. Chem. Phys. **127**, 104710 (2007).
[41]M. Zavelani-Rossi, M. G. Lupo, F. Tassone, L. Manna, and G. Lanzani, Nano Lett. **10**, 3142 (2010).
[42]N. J. Borys, M. J. Walter, J. Huang, D. V. Talapin, and J. M. Lupton, Science **330**, 1371 (2010).
[43]W. A. Harrison, E. A. Kraut, J. R. Waldrop, and R. W. Grant, Phys. Rev. B **18**, 4402 (1978).
[44]E. R. Smith, J. M. Luther, and J. C. Johnson, Nano Lett. **11**, 4923 (2011).
[45]L. Amirav and A. P. Alivisatos, J. Phys. Chem. Lett. **1**, 1051 (2010).
[46]C. L. Choi, H. Li, A. C. K. Olson, P. K. Jain, S. Sivasankar, and A. P. Alivisatos, Nano Lett. **11**, 2358 (2011).
[47]Z. Deutsch, O. Schwartz, R. Tenne, R. Popovitz-Biro, and D. Oron, Nano Lett. **12**, 2948 (2012).
[48]E. A. Dias, J. I. Saari, P. Tyagi, and P. Kambhampati, J. Phys. Chem. C **116**, 5407 (2012).